Supporting Information

Well-defined hollow tube@sheets $NiCo_2S_4$ core-shell nanoarrays for ultrahigh capacitance supercapacitor

Jiachao Zhou, Yingchao Wang, Jiaojiao Zhou*, Kang Chen, Lei Han*

State Key Laboratory Base of Novel Functional Materials and Preparation Science, School of Materials Science and Chemical Engineering, Ningbo University, Ningbo, Zhejiang 315211, China. Email: hanlei@nbu.edu.cn

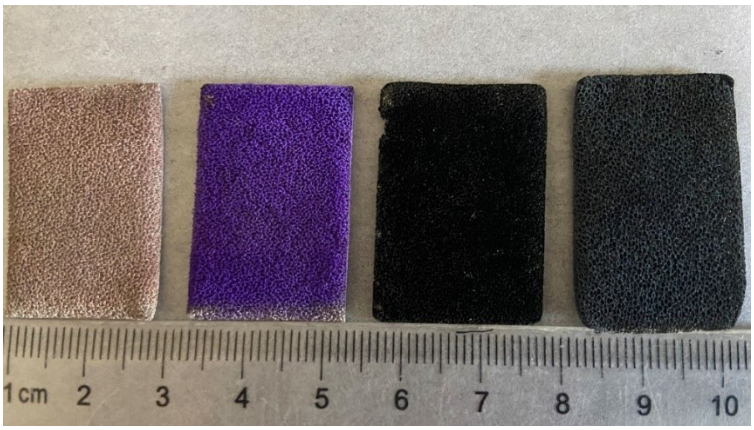

Fig. S1. Photography of CoCH, CoCH@ZIF-67, Co_9S_8, $NiCo_2S_4$ on the Ni Foam.

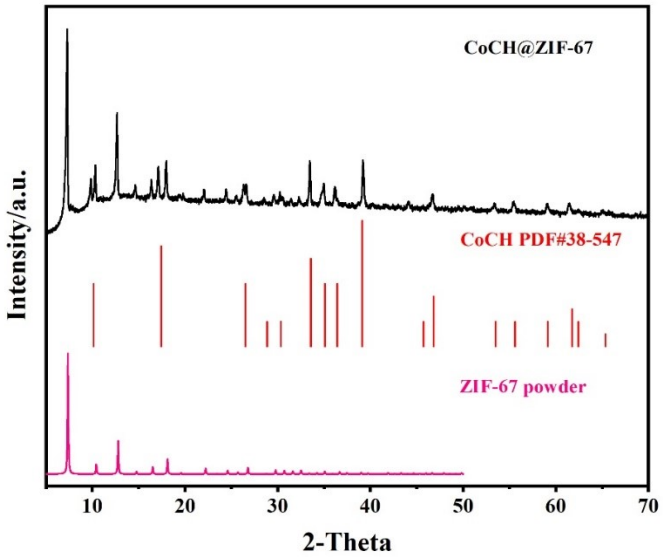

Fig. S2. XRD pattern of CoCH@ZIF-67.

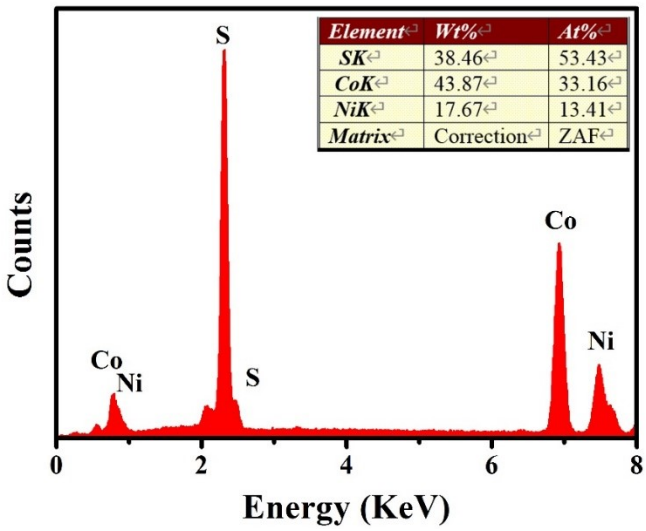

Fig. S3. EDS of $NiCo_2S_4$/NF.

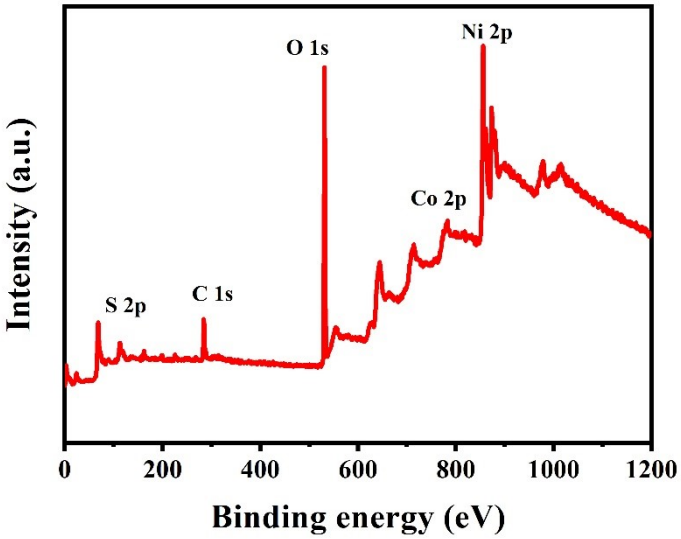

Fig. S4. Survey spectra of $NiCo_2S_4$/NF.

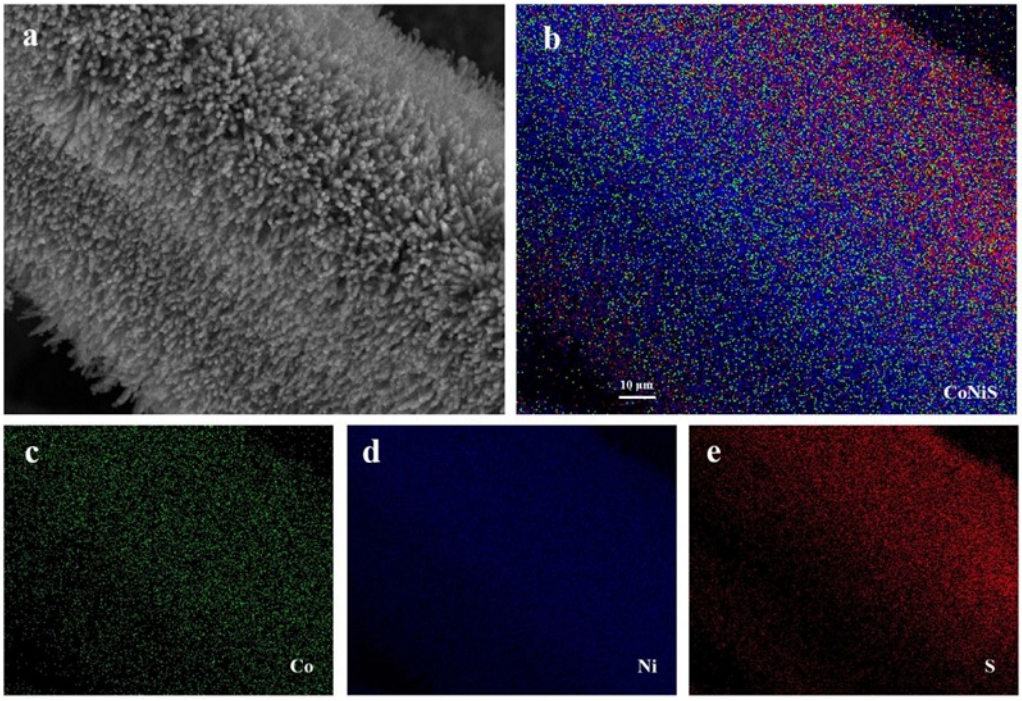

Fig. S5. The overall distribution of elements of $NiCo_2S_4$/NF

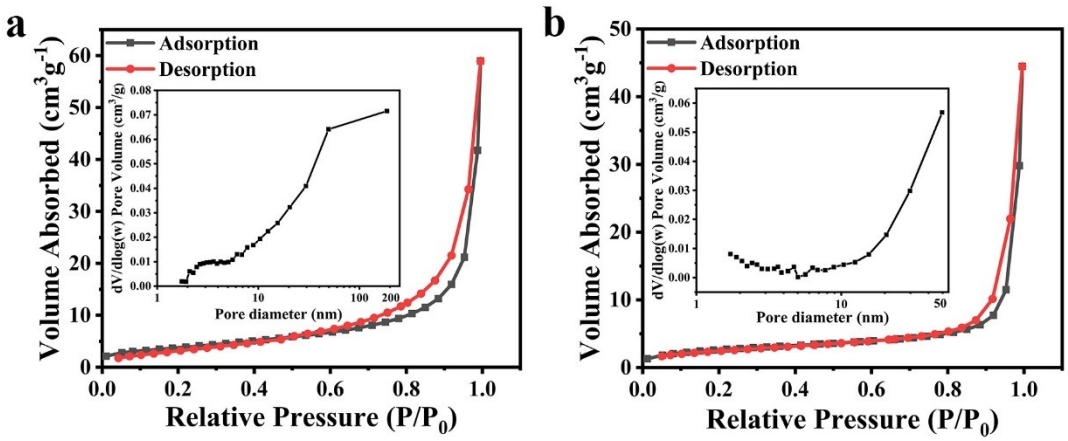

Fig. S6. (a) N_2 adsorption-desorption isotherm curve and pore size distribution curve of $NiCo_2S_4$/NF. (b) N_2 adsorption-desorption isotherm curve and pore size distribution curve of Co_9S_8/NF.

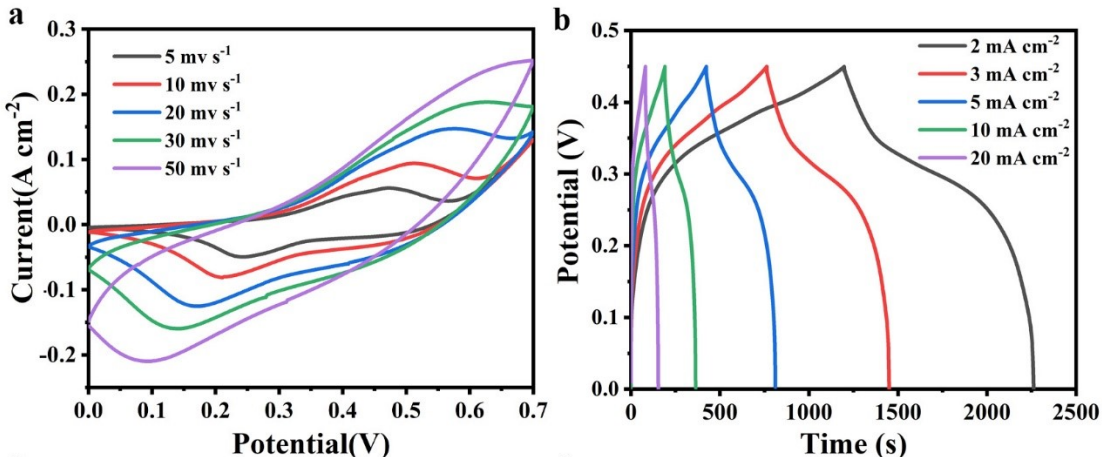

Fig. S7. (a) CV curves of Co_9S_8/NF at different scan rates; (b) GCD curve of Co_9S_8/NF at different current densities.

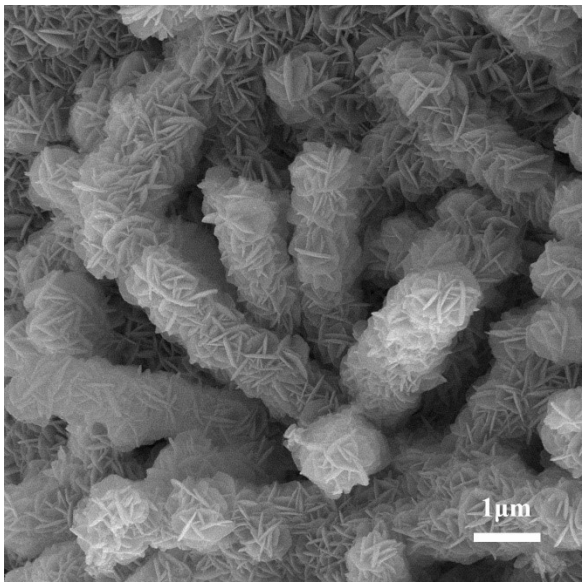

Fig. S8. SEM image of $NiCo_2S_4$/NF after cycling test.

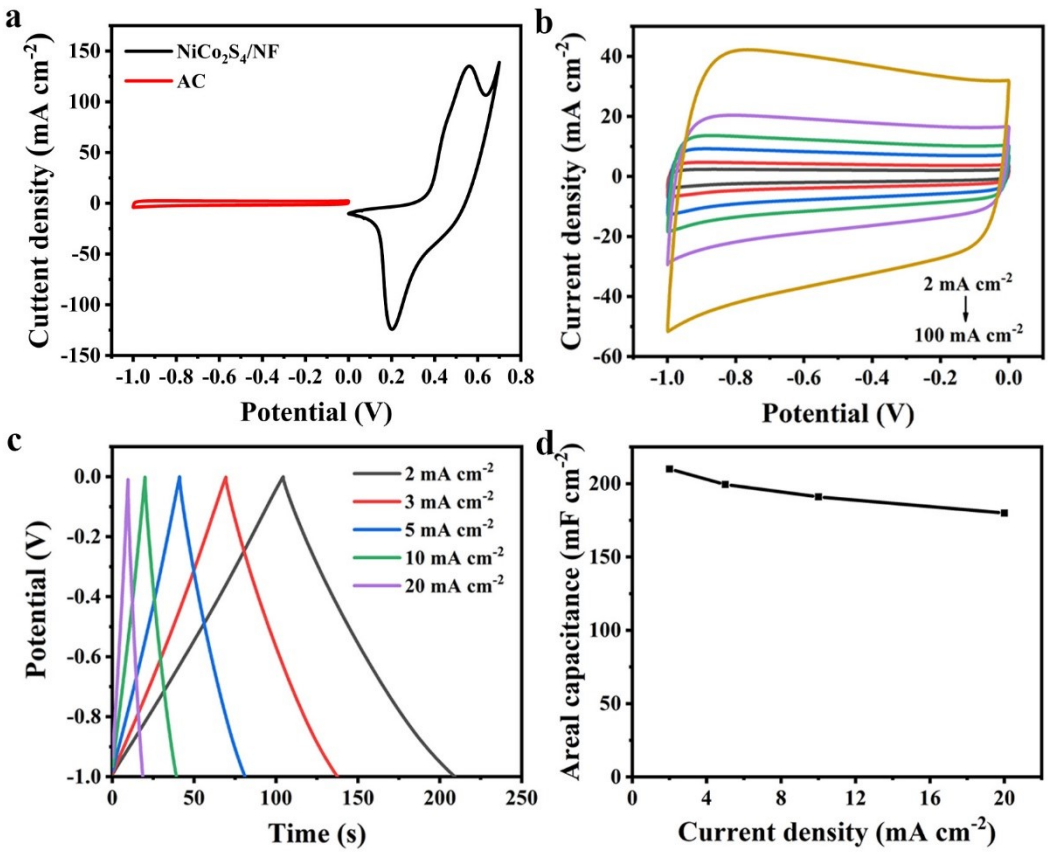

Fig. S9. (a) CV curves of $NiCo_2S_4$/NF and AC at a scan rate of 5 mV s^{-1}; (b) CV curves of AC at different scan rates; (c) GCD curves of AC at different current densities; (d) Specific capacitances of AC.

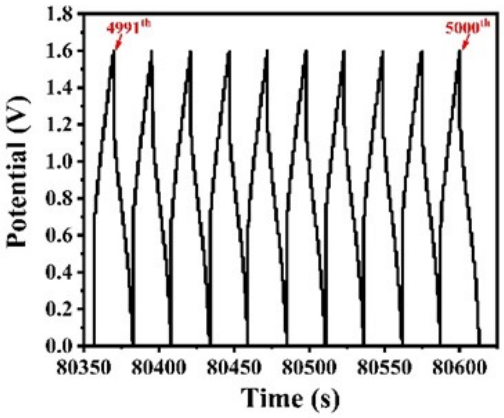

Fig. S10. Cycling performance of ACS device.